Tribology and Materials
Vol. x, No. x, 202x, pp. xx-xx

ISSN 2812-9717
https://doi.org/10.46793/tribomat.202x.xxx

Optimisation of base oil production from sunflower oil and trimethylolpropane via response surface methodology

Nurazira Mohd NOR [1,*], Muhammad Muizzuddin KHAIRUDDIN [1], Asiah ABDULLAH [1], Sheikh Ahmad Izaddin Sheikh Mohd GHAZALI [1], Is FATIMAH [2], Nur Sulihatimarsyila Abd WAFTI [3]

[1] Universiti Teknologi MARA, Cawangan Negeri Sembilan, Kampus Kuala Pilah, Kuala Pilah, Malaysia
[2] Universitas Islam Indonesia, Yogyakarta, Indonesia
[3] Malaysian Palm Oil Board, Kajang, Malaysia
*Corresponding author: nurazira@uitm.edu.my

Keywords
esterification
D-optimal design
trimethylolpropane
sunflower oil
polyolester
biolubricant

History
Received: 12-01-2026
Revised: 10-05-2026
Accepted: 01-06-2026

Abstract

Biolubricants are derived from renewable sources. They offer a more environmentally friendly alternative to conventional petroleum-based lubricants. The biolubricant base was synthesised from unsaturated fatty acids derived from sunflower oil (SFOUFA) via esterification with trimethylolpropane (TMP) to produce sunflower oil unsaturated fatty acids trimethylolpropane ester (SFOUFATMPE). In this study, response surface methodology (RSM) using D-optimal design was employed to optimise the esterification process. The range of parameters used was SFOUFA : TMP mole ratio (3.0 to 4.5 mol/mol), catalyst amount (0.5 to 3.0 wt. %), reaction time (3 to 7 h) and reaction temperature (130 to 170 °C). The optimum reaction conditions were determined as an SFOUFA : TMP mole ratio of 4.0 mol/mol, 1.13 wt. % H_2SO_4 catalyst, a reaction time of 6 hours and a reaction temperature of 154 °C, which produced a 79.41 % yield of SFOUFATMPE. The SFOUFATMPE showed a flash point of 290 °C, a pour point of −18 °C and an oxidative stability of 24 minutes. These properties indicate that SFOUFATMPE has potential as a biolubricant. However, further chemical modification is required to improve its oxidative stability for commercial lubricant applications.

1. Introduction

Lubricants play an essential role in reducing friction and wear between moving parts in machines, thereby improving their performance [1,2]. Usually, the lubricant consists of 70 to 99 % base oil, with the remainder consisting of additives to improve its performance [3]. Mineral oil derived from petroleum is commonly used as a base oil in the production of lubricants. However, mineral oil comes from non-renewable sources and has a negative impact on the environment.

One of the alternatives nowadays is the increasing use of bio-based lubricants, also known as biolubricants, which aim to reduce the reliance on petroleum-derived lubricants. Biolubricants are typically made from sources such as plant oils, waste cooking oils and animal fats. This makes them biodegradable and non-toxic to the environment, unlike mineral oil-based lubricants [4]. Biolubricants are suitable for applications including metalworking, aviation, hydraulics, construction, machinery, vehicles and marine equipment [5].

Biolubricants derived from plant oils exhibit several advantageous lubrication properties, including a low pour point due to a high degree of unsaturation, a high flash point that provides resistance to fire hazards and a high viscosity index often linked to saturated fatty acid content [2,5]. Despite these characteristics, plant oils cannot be used directly as biolubricants because they are not very stable when it comes to heat and oxygen due

to the presence of hydrogen atoms located on the central glycerol backbone of the triacylglycerol molecule [6,7]. At high temperatures, these hydrogen atoms act as active oxidative sites, making plant oils more easily degraded and thermally unstable. During oxidative degradation, the removal of hydrogen can cause the formation of olefins (unsaturated compounds) and acids. The resulting unsaturated compounds may undergo polymerisation, leading to increased oil viscosity and the formation of precipitates [4,8].

Various chemical modifications have been developed to overcome the limitations of the low oxidative stability of plant oils. Among the most commonly employed methods is esterification with polyhydric alcohol due to its simplicity, feasibility and cost-effectiveness. Polyhydric alcohols are considered a preferred method for biolubricant production, as they have been reported in numerous studies to yield high conversion rates. Polyhydric alcohols, such as neopentyl glycol, trimethylolpropane (TMP), and pentaerythritol, are often used in the production of biolubricants, commonly referred to as polyolesters. These alcohols are selected because they lack beta-hydrogen atoms. This makes them ideal substitutes for glycerol as a molecular backbone [9].

In recent years, researchers have investigated the use of TMP in producing biolubricants through esterification and transesterification of various bio-based feedstocks. Sulfuric acid is commonly used as a catalyst because it provides high reaction efficiency and produces high ester yield. One study conducted by Jamaluddin et al. [10] used fatty acids derived from corn oil, reacting them with TMP in the presence of sulfuric acid. This reaction achieved an impressive 97.9 % yield, and the resulting ester exhibited a pour point of –20 °C and a flash point of 300 °C. Another study conducted by Ramos et al. [11] used oleic acid as the base material, in which TMP esters were synthesised via acid-catalysed esterification. The researchers developed predictive models for viscosity and viscosity index, with the di- and triesters achieving viscosity index values of up to 218, suggesting excellent performance for lubrication applications.

The esterification reaction was optimised using response surface methodology (RSM) by employing D-optimal design. RSM serves as a statistical tool to evaluate the influence of variables and their interactions to achieve an efficient optimisation process. Among its key advantages are reduced experimental time and lower chemical consumption. Compared to other experimental designs, the D-optimal design is particularly advantageous as it minimises parameter covariance by maximising the determinant of the information matrix [12,13].

The objective of this study is to synthesise a biolubricant base from unsaturated fatty acids derived from sunflower oil (SFO) through an esterification reaction with TMP. The optimisation of the esterification process was carried out using the D-optimal design to maximise the percentage yield of the final product, known as sunflower oil unsaturated fatty acids trimethylolpropane ester (SFOUFATMPE). The functional groups and chemical structure of the synthesised ester were characterised using Fourier transform infrared spectroscopy (FTIR) and nuclear magnetic resonance (NMR) spectroscopy. In addition, the lubrication properties of SFOUFATMPE were evaluated to assess its performance as a biolubricant base.

2. Materials and methods

2.1 Materials

Sunflower oil was purchased from Melbelle Natural (Malaysia). Trimethylolpropane (98 %) was purchased from Shanghai Macklin Biochemical (China). Sulfuric acid, toluene, ethyl acetate, sodium bicarbonate, sodium chloride, sodium sulfate, hydrochloric acid, *n*-hexane, potassium hydroxide and ethanol were purchased from Systerm Chemicals (Malaysia). All chemicals were analytical reagents and used without further purification.

2.2 Synthesis of biolubricant

SFO was initially hydrolysed to obtain sunflower oil fatty acids (SFOFA) using 2.3 mol/m^3 ethanolic potassium hydroxide at 50 °C for 0.97 hours, following the method described by Khairuddin et al. [14]. After hydrolysis, saturated and unsaturated fatty acids were separated using the low-temperature crystallisation technique. The process involved a methanol-to-fatty acid ratio of 15 : 1 wt. %/wt. % at a temperature of –15 °C for 24 hours, as reported by Khairuddin et al. [15], to obtain SFOSFA and SFOUFA. Fatty acid compositions in SFOSFA and SFOUFA were determined using gas chromatography-mass spectrometry.

The esterification of SFOUFA with TMP was conducted to produce SFOUFATMPE as a biolubricant base, following the method reported by Nor et al. [9] with slight modifications. The reaction was performed in a 250 ml three-neck round-bottom flask equipped with a Dean-Stark apparatus, a reflux condenser, a magnetic stirrer and a thermometer. Toluene was gradually added at a rate of 20 ml every 30 minutes as an azeotropic agent to facilitate the removal of water formed as a byproduct, ensuring the completion of the esterification process. Upon completion of the reaction, the mixture was allowed to cool to room temperature, then dissolved in 20 ml of ethyl acetate and transferred into a 250 ml separatory funnel. Then, 20 ml of saturated sodium hydrogen carbonate was added to neutralise any remaining acid, followed by the addition of 20 ml of saturated sodium chloride to prevent emulsion formation.

The mixture was shaken and allowed to separate into two distinct layers, where the upper layer was the organic phase and the lower layer was the aqueous phase. The aqueous phase was discarded and the washing steps were repeated until a neutral pH was achieved. The organic layer was then collected and dried using anhydrous sodium sulphate to remove any remaining water. The solvent was subsequently removed using a rotary evaporator and the final product, SFOUFATMPE, was collected for further analysis. The yield of SFOUFATMPE was calculated based on the mass of the isolated final product.

2.3 Optimisation process for esterification

The esterification parameter ranges were selected based on preliminary screening conducted prior to the optimisation study. Four key parameters were identified as having significant effects on the esterification process: mole ratio of SFOUFA to TMP, catalyst amount, reaction time and reaction temperature, as presented in Table 1. The selected ranges for these variables were as follows: mole ratio of SFOUFA to TMP from 3.0 to 4.5, catalyst amount from 0.5 to 3.0 wt. %, reaction time between 3 and 7 hours and reaction temperature from 130 to 170 °C. The percentage yield of SFOUFATMPE was used as the response variable. Based on these parameters and their levels, the D-optimal design generated 25 experimental runs to optimise the esterification reaction. Each experiment was conducted according to the specific conditions recommended by the design model.

Table 1. Parameters and their levels for D-optimal design for the esterification reaction

Parameter	Unit	Level		
		−1	0	+1
SFOUFA : TMP mole ratio (A)	–	3.0	3.75	4.5
Catalyst amount (B)	wt. %	0.5	1.75	3.0
Reaction time (C)	h	3	5	7
Reaction temperature (D)	°C	130	150	170

2.4 Characterisation of biolubricant

Gas chromatography-flame ionisation detection analysis was also performed to determine the ester composition of the synthesised product. The functional groups of the synthesised product (SFOUFATMPE) were identified using attenuated total reflectance Fourier transform infrared spectroscopy (FTIR). The analysis was carried out using a PerkinElmer Spectrum GX FTIR spectrometer in the range of 4000 to 650 cm^{-1} to confirm the formation of ester bonds and to detect the presence of characteristic peaks corresponding to specific functional groups. Nuclear magnetic resonance (NMR) spectroscopy was used to confirm the chemical structure of the synthesised product. Proton (^{1}H) NMR was recorded at 400 MHz and carbon (^{13}C) NMR at 100.61 MHz using a JEOL-ECP 400 spectrometer. Approximately 25 mg of the sample was dissolved in deuterated chloroform.

Physicochemical properties of the biolubricant base were characterised according to standard ASTM methods. The pour point was measured using the ASTM D97 method with a U-tube as the sample container. The filled U-tube was kept in a freezer at −30 °C for 24 hours and the temperature at which the sample started to flow was recorded as the pour point. The flash point of SFO was measured using the ASTM D92 method by heating 2 ml of it in a crucible on a hot plate. The temperature at which a flame first appeared was recorded as the flash point. Pour point and flash point were performed in triplicate.

The oxidative stability was analysed using the rotating pressure vessel oxidation test (RPVOT) according to ASTM D2272, in which the sample, mixed with a copper catalyst, was sealed in a steel vessel, pressurised with oxygen at 0.6206 MPa and

heated to 150 °C. The time required for a 0.172 MPa pressure drop was recorded as the oxidation induction time, indicating the lubricant's resistance to oxidation. Kinetic viscosity at 40 and 100 °C, viscosity index and rheological behaviour were examined using an Anton Paar Physica MCR 301 rheometer with cone-and-plate geometry (CP 25-2, 0.051 mm gap) at 25 °C over a shear rate range of $0 - 100\ s^{-1}$ to determine whether the sample exhibited Newtonian or non-Newtonian flow behaviour.

3. Results and discussion

3.1 Synthesis of SFOUFATMPE

Sunflower oil (SFO) was initially hydrolysed using ethanolic potassium hydroxide to produce sunflower oil fatty acids (SFOFA), following the method reported by Khairuddin et al. [14]. The hydrolysis process consisted of two main steps. The first step involved saponification, in which fatty acids were separated from the glycerol backbone by converting SFO into its potassium salt form (fatty acid potassium salt). This was followed by an acidification step to convert the potassium salts into free fatty acids (SFOFA), resulting in a yield of 96 %.

Following hydrolysis, SFOFA was separated into saturated (SFOSFA) and unsaturated fatty acids (SFOUFA) using a methanol crystallisation technique, as described by Khairuddin et al. [15]. The separation resulted in the saturated fraction (SFOSFA) appearing as a solid at room temperature with a yield of 8.32 % and a purity of saturated fatty acids greater than 99 %. The unsaturated fraction (SFOUFA) remained in liquid form at room temperature, with a yield of 85.72 % and a purity of 98 % unsaturated fatty acids. The purity of the fatty acid composition in SFOSFA and SFOUFA was determined by gas chromatography-mass spectrometry analysis. The recovered SFOUFA was then subjected to esterification with TMP and a polyhydric alcohol to produce SFOUFATMPE.

The process was optimised using RSM based on a D-optimal design to maximise the percentage yield of SFOUFATMPE, which served as the response variable. The experimental design employed a three-level factorial structure involving four key reaction parameters: mole ratio of SFOUFA to TMP (A), catalyst amount (B), reaction time (C) and reaction temperature (D). The D-optimal design generated 25 experimental runs and the corresponding predicted response values, as presented in Table 2. The predicted value was generated from the RSM using the experimental results. Statistical analysis of the yield data was performed, and the effects of the individual parameters and their interactions were visualised using various plots. These included 3D surface response plots and corresponding contour plots to illustrate the influence of the four independent variables. In addition, empirical and mathematical models were developed and optimised using RSM software to identify the optimal reaction conditions.

Table 2. Experimental runs from D-optimal design and the percentage yield of SFOUFATMPE

Run	Parameter				Response: Yield, %	
	A	B, wt. %	C, h	D, °C	actual	predicted
1	3.0	1.3	3	130	53.31	53.99
2	3.5	1.8	5	153	76.40	77.95
3	3.5	3.0	3	130	60.00	60.53
4	4.5	2.5	3	130	47.00	47.16
5	3.5	0.5	5	130	56.81	56.24
6	3.9	0.5	7	170	71.39	71.28
7	3.5	2.5	3	130	59.78	59.38
8	3.0	0.7	3	170	54.50	54.22
9	3.5	3.0	3	130	61.00	60.53
10	3.0	0.7	7	130	59.00	58.03
11	3.9	2.5	7	170	76.00	76.99
12	3.0	3.0	7	130	50.00	50.09
13	3.9	1.8	3	153	72.00	70.20
14	3.9	2.5	7	170	78.50	76.99
15	3.9	2.5	3	170	60.50	61.90
16	3.5	1.3	5	154	79.10	78.35
17	3.0	0.5	7	170	52.00	52.40
18	3.5	2.5	5	153	75.96	75.62
19	3.0	0.7	3	170	54.50	54.22
20	3.5	2.5	7	153	75.38	75.66
21	3.9	0.5	7	170	71.38	71.28
22	3.5	0.5	7	130	55.00	55.91
23	3.5	3.0	3	170	40.60	40.11
24	3.5	0.7	3	153	67.90	68.84
25	4.5	1.8	5	153	78.00	78.10

The percentage yield of SFOUFATMPE from the esterification process was evaluated based on

individual reaction parameters suggested by the D-optimal design. The discussion focuses on the effects of the esterification variables. The percentage yield of SFOUFATMPE obtained from the esterification reactions ranged from a minimum of 40.11 % to a maximum of 78.35 %. The D-optimal model analysis showed that the yield responded well to the selected reaction parameters.

A Box-Cox transformation was performed to evaluate the normality and stability of the model. In the Box-Cox transformation, the lambda (λ) value generally ranges from −3 to +3, where λ = 1 indicates no transformation, λ = 0 represents logarithmic transformation, and other positive and negative values correspond to the different power transformations. The optimal λ value obtained was 1.64669, indicating that the data were normally distributed and did not require a significant transformation. The low maximum-to-minimum ratio of lambda shows that the Box-Cox transformation had little effect, meaning the model is reliable. This justifies using the original yield values without transformation. The strong match between experimental and predicted results confirms that the D-optimal design worked well. Overall, the quadratic model from RSM was suitable for optimising the esterification process, with no signs of model errors.

The perturbation plot on Figure 1 illustrates the individual effect of each parameter: A (SFOUFA : TMP mole ratio), B (catalyst amount), C (reaction time) and D (reaction temperature) on the percentage yield of SFOUFATMPE, while keeping other variables constant at the reference point (A = 3.75, B = 1.75 wt. %, C = 5 h, D = 150 °C). In the graph, parameter B shows the steepest slope near the reference point, indicating that catalyst amount has the most significant influence on yield. Parameters A and D also show noticeable curvature, suggesting their impact is nonlinear. Both higher and lower deviations from the centre reduce the yield. The decrease in yield noticed at high temperatures, near 170 °C, is due to the thermal degradation of the unsaturated fatty acids. Meanwhile, parameter C displays the flattest curve, indicating that reaction time has the least effect on the yield within the studied range. Overall, the plot confirms that precise optimisation of catalyst amount, followed by the mole ratio and temperature, is crucial for maximising the esterification yield.

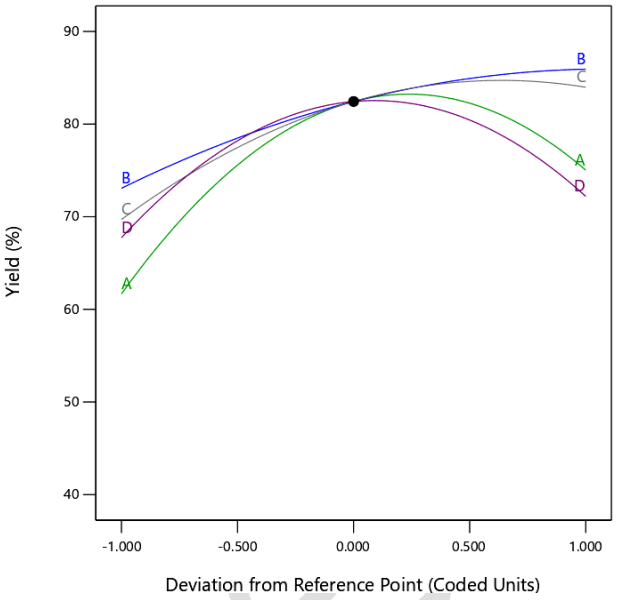

Figure 1. Perturbation effect plot of all parameters for percentage yield SFOUFATMPE by D-optimal design

The plots of residuals versus run, actual versus predicted and the normal plot of residuals are shown in Figure 2, where the colours in the plots are based on the RSM model and represent the variation in the predicted response. The residuals versus run plot (Fig. 2a) demonstrates that the residuals are randomly scattered around the zero line. This suggests that the errors are independent and that the assumption of constant variance is satisfied. Furthermore, all residual values lie within the control limits of ±4.29681, indicating the absence of outliers or influential data points. This confirms that the model is statistically adequate and that no significant anomalies are present in the dataset. The normal plot of residuals (Fig. 2b) shows that most points lie close to a straight line, indicating that the residuals are normally distributed. This suggests that the model meets the assumption of normality, with no clear signs of outliers. The good alignment of points confirms that the model is statistically reliable and that no transformation of the response variable is needed. The predicted versus actual plot (Fig. 2c) shows a strong linear correlation, with most data points closely aligning with the 45-degree reference line. This indicates excellent agreement between the experimental and predicted values, reflecting the high predictive accuracy of the model. The distribution of experimental points across various parameter combinations also aligns well, reinforcing the robustness and validity of the quadratic model developed using the D-optimal RSM design to optimise the esterification process.

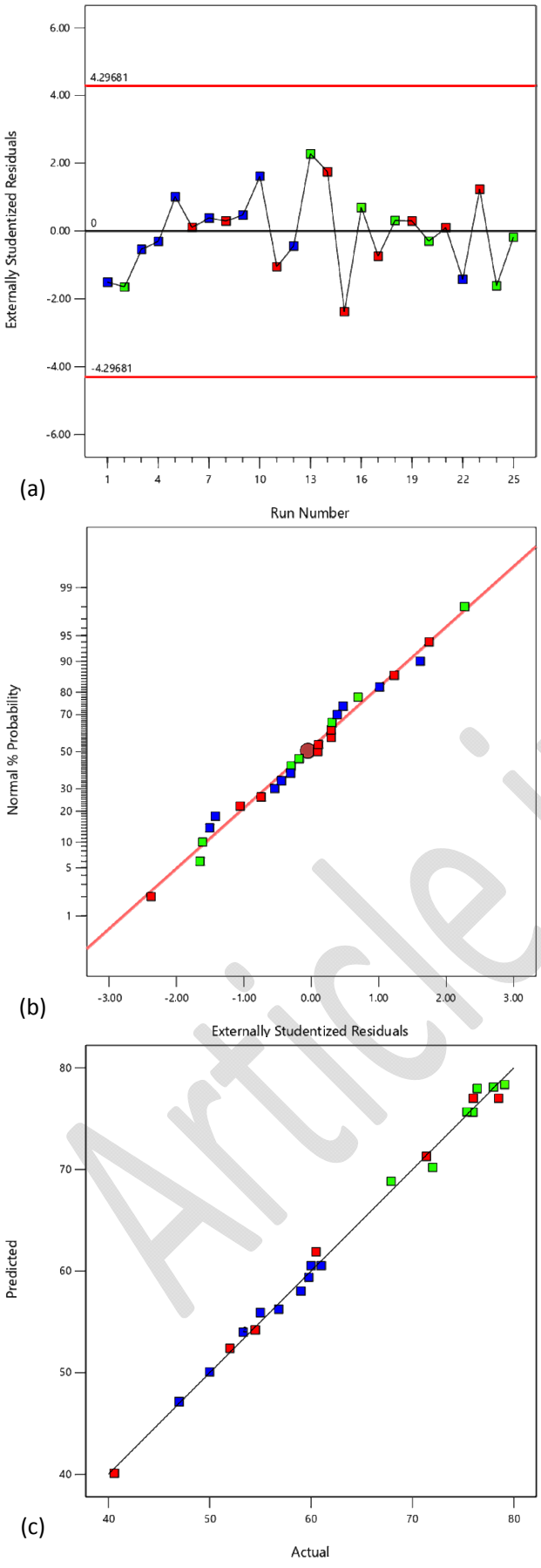

Figure 2. Percentage yield of SFOUFATMPE: (a) residuals versus run, (b) normal plot of residuals and (c) predicted versus actual

3.2 D-optimal design fitting

The analysis of variance (ANOVA) indicates that the developed model is highly significant, with a p-value of < 0.0001, well below the 0.05 threshold. The high F-value of 133.52 further supports the model's significance, indicating that the variation explained by the model is much greater than the unexplained (error) variation. There is only a 0.01 % probability that this large F-value could be due to random noise, confirming the reliability of the model. The coefficient of determination (R^2) of 0.9947 indicates that 99.47 % of the variation in the response is explained by the model. The adjusted R^2 (0.9872) and predicted R^2 (0.9449) are both close to the R^2 value and differ by less than 0.2, suggesting excellent agreement and model predictability. The adequate precision value of 38.6245, which is well above the recommended minimum of 4, indicates a strong signal-to-noise ratio. Additionally, the coefficient of variation is low at 2.01 % and the standard deviation is 1.28, reflecting high model precision and consistency. The lack-of-fit test yielded a p-value of 0.2154, which is not significant (p > 0.05), confirming that the model fits the data well and that no substantial lack of fit exists. The quadratic regression model for predicting the percentage yield of SFOUFATMPE is presented in the following equation.

$$\begin{aligned}\text{Yield} = {} & 82.44 + 6.68\,A + 6.43\,B + 7.14\,C + \\ & 2.23\,D + 21.69\,AB + 6.44\,AC + 13.03\,AD + \\ & 1.52\,BC - 9.89\,BD - 1.79\,CD - 14.09\,A^2 - \\ & -2.94\,B^2 - 5.60\,C^2 - 12.47\,D^2. \end{aligned} \quad (1)$$

ANOVA analysis from Table 3 reveals that all four main reaction parameters, which were SFOUFA:TMP mole ratio (A), catalyst amount (B), reaction time (C) and reaction temperature (D), have significant effects on the percentage yield of SFOUFATMPE. Their respective p-values are all below 0.05, with A, B and C showing extremely strong significance (p < 0.0001), and D also showing significance with a p-value of 0.0016. This indicates that all individual parameters have a statistically meaningful impact on the esterification process. For the interaction terms, all combinations (A×B, A×C, A×D, B×C, B×D and C×D) are also significant (p < 0.05), suggesting that the interactions between variables significantly influence the response. In particular, the interactions A×B, A×C, A×D and B×D show very high significance (p < 0.0001), highlighting strong

synergistic effects among these parameters. For the quadratic terms, A square, C square, D square, A×A, C×C and D×D are all highly significant with p-values less than 0.0001, suggesting strong curvature effects on the yield. These results validate the use of a quadratic model to accurately describe the system behaviour and optimise the reaction conditions [9].

3.3 Response surface analysis

The interaction effect between the reaction variables on the percentage yield SFOUFATMPE can be demonstrated with the 3D surface plots. The interaction between mole ratio and catalyst amount (Fig. 3a) shows a steep incline, indicating a strong influence of both variables on the yield. As the mole ratio and catalyst amount increase, the yield rises significantly before levelling off slightly, suggesting a saturation point. This means that while both variables promote the reaction, excessive levels may not provide further improvement. The accompanying contour plot shows a distinct gradient that transitions from green to red as both variables increase. Closely spaced contours in the lower range imply a highly sensitive region, where small changes in either parameter led to significant shifts in yield.

The 3D plot of mole ratio versus reaction time (Fig. 3b) shows a curved surface, with the yield improving with increasing values of both parameters up to a certain point. Beyond that, the yield either declines or remains constant, indicating an optimal reaction window. This suggests that extended reaction time or an overly high mole ratio may not necessarily enhance the result and could potentially lead to inefficiencies. The corresponding contour plot shows a smooth, oval-shaped pattern with its peak yield centred around a mole ratio of 3.5 to 4.0 and a reaction time of about 5 to 6 hours. This area is highlighted in red, pointing to the best conditions for maximising yield.

When analysing the interaction between mole ratio and reaction temperature (Fig. 3c), the 3D surface plot takes on a dome-like shape. Yield initially increases as both parameters increase, but it begins to decline once the temperature exceeds a threshold. This may be due to thermal degradation or negative side reactions that occur at higher temperatures. The contour plot supports this observation, with the highest yield zone occurring around a mole ratio of 4.0 and a reaction temperature of 160 – 165 °C. The gradual shift in colour and contour curvature suggests that exceeding the optimal range can lead to diminishing responses, emphasising the need for careful temperature control.

Table 3. ANOVA analysis data for the percentage yield of SFOUFATMPE

Source	Sum of squares	Degree of freedom	Mean square	F-value	p-value	Status
Model	3052.78	14	218.06	133.52	< 0.0001	significant
A	160.32	1	160.32	98.16	< 0.0001	significant
B	121.48	1	121.48	74.39	< 0.0001	significant
C	261.76	1	261.76	160.28	< 0.0001	significant
D	30.13	1	30.13	18.45	0.0016	significant
A×B	257.94	1	257.94	157.94	< 0.0001	significant
A×C	94.58	1	94.58	57.92	< 0.0001	significant
A×D	254.34	1	254.34	155.74	< 0.0001	significant
B×C	13.76	1	13.76	8.43	0.0158	significant
B×D	324.94	1	324.94	198.97	< 0.0001	significant
C×D	19.39	1	19.39	11.87	0.0063	significant
A×A	289.99	1	289.99	177.57	< 0.0001	significant
B×B	6.74	1	6.74	4.13	0.0695	
C×C	64.85	1	64.85	39.71	< 0.0001	significant
D×D	196.55	1	196.55	120.35	< 0.0001	significant
Lack-of-fit	12.71	6	2.12	2.34	0.2154	

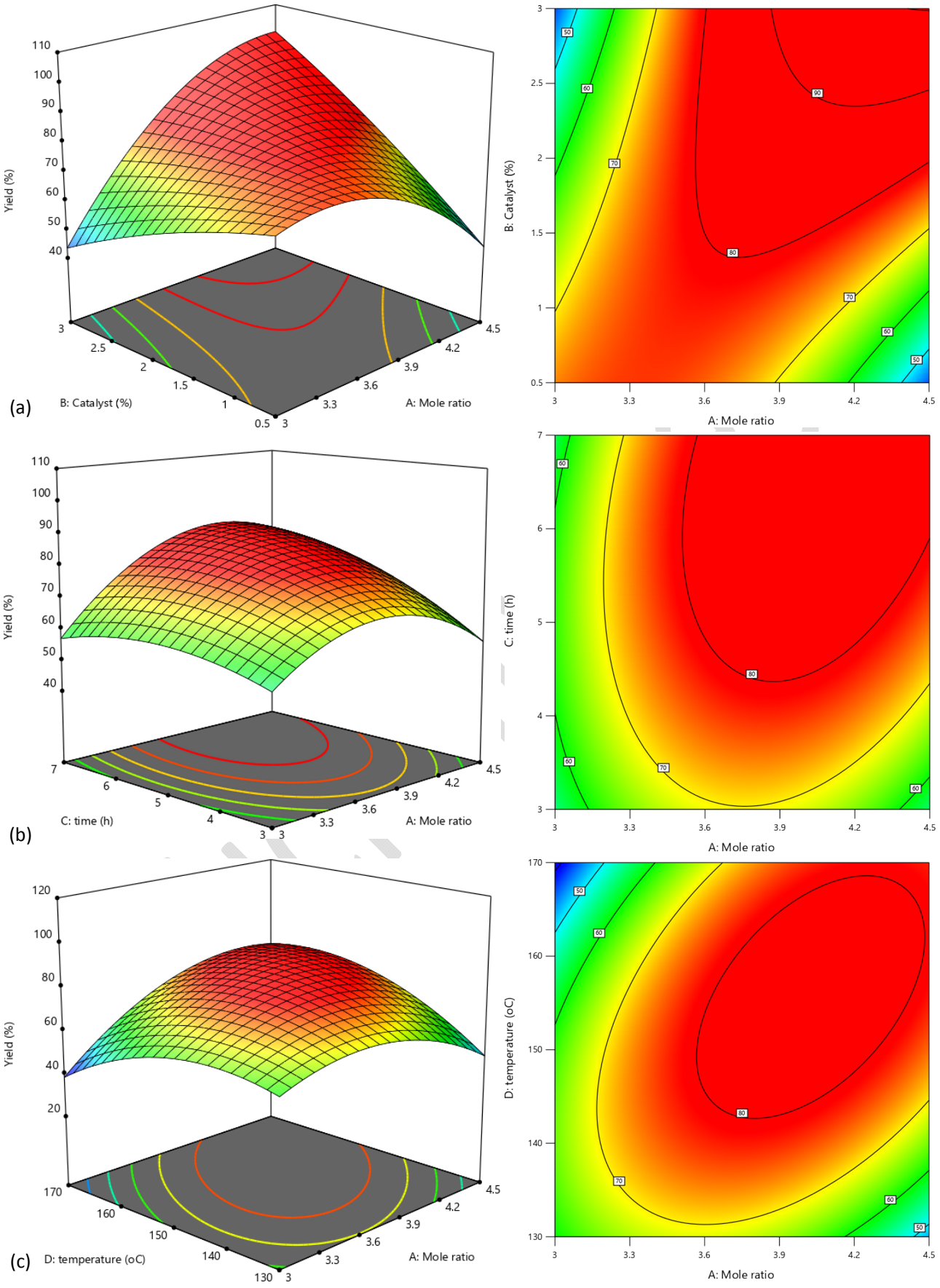

Figure 3. 3D surface and contour plots of SFOUFATMPE percentage yield for different parameters interaction: (a) SFOUFA : TMP mole ratio vs catalyst amount, (b) SFOUFA : TMP mole ratio vs reaction time, (c) SFOUFA : TMP mole ratio vs reaction temperature, (d) catalyst amount vs reaction time, (e) catalyst amount vs reaction temperature and (f) reaction time vs reaction temperature

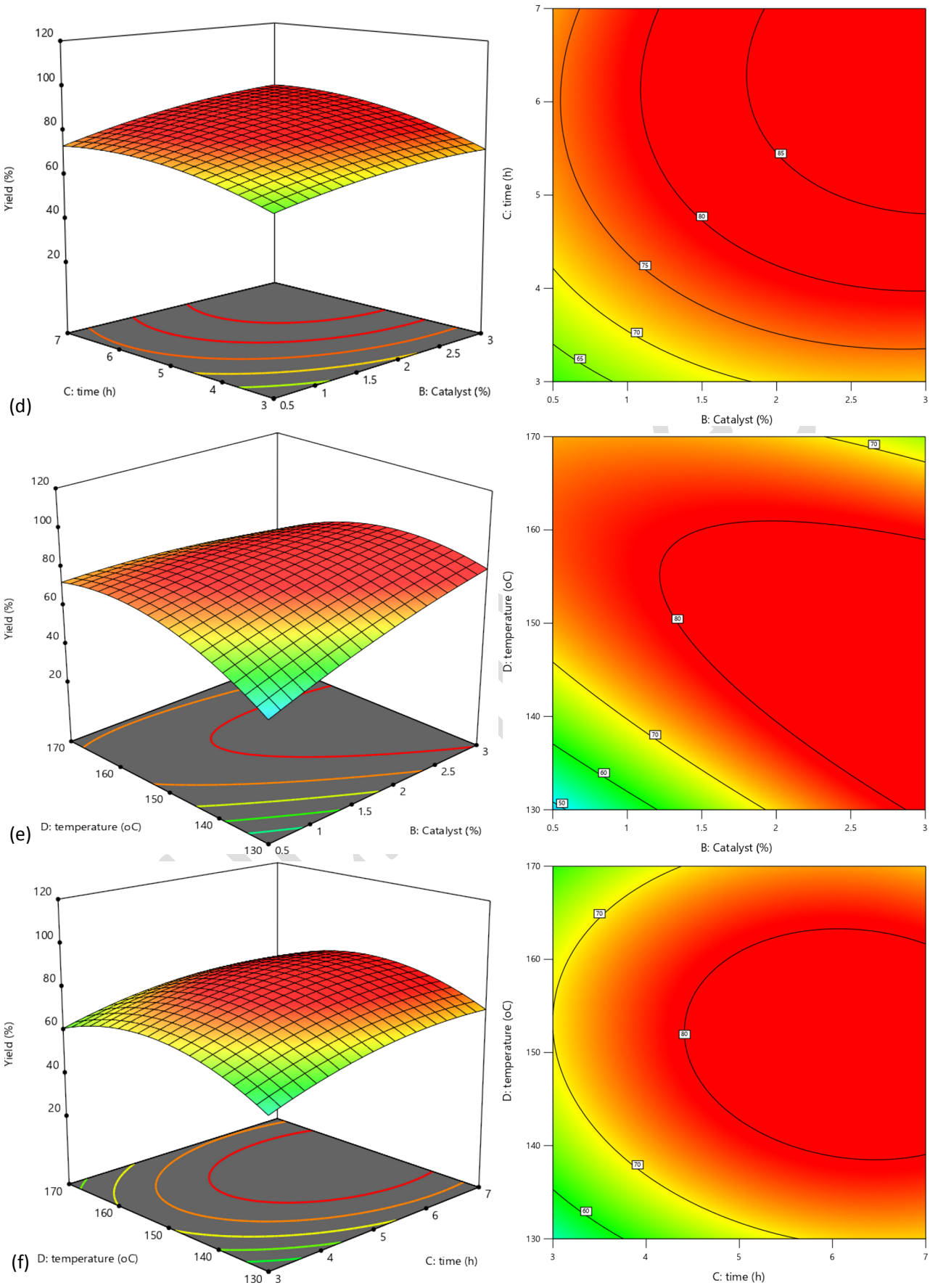

Figure 3. *Continued*

The 3D plot of catalyst amount and reaction time (Fig. 3d) shows a relatively flat surface along the catalyst amount axis, indicating that catalyst amount has a limited effect on yield over this range.

In contrast, reaction time shows a more pronounced influence, with the yield steadily increasing as time increases. This means that longer reaction durations are more critical in this interaction. The contour plot further highlights this trend, with contour lines more curved and closer together along the reaction time axis, while remaining widely spaced along the catalyst amount axis. Thus, focusing on reaction duration appears more beneficial than increasing catalyst concentration.

In the 3D surface plot of catalyst amount and reaction temperature (Fig. 3e), the yield gradually increases with both variables, but the slope becomes gentler at higher values. This implies a moderate influence from both parameters, with a tendency to plateau. The contour plot exhibits a narrow red zone, representing the region of highest yield. The elliptical shape of the contours suggests that both catalyst amount and reaction temperature must be carefully balanced to achieve optimal results. A small deviation from this ideal range could result in a noticeable decrease in performance, highlighting the system's sensitivity to changes in these two variables.

For the reaction time and reaction temperature interaction (Fig. 3f), the 3D surface plot shows a ridge-like increase in yield, which peaks at intermediate values of both variables. The yield tends to increase with longer reaction times and moderately high temperatures, but excessive reaction temperatures do not provide additional benefit and may even reduce the yield. The contour plot clearly illustrates this trend, with closely spaced lines along the reaction temperature axis, indicating a sharper response to changes in reaction temperature than to changes in reaction time. The best region appears to lie around 5 to 6 hours of reaction time and approximately 160 °C reaction temperature, indicating the most efficient conditions for maximising yield.

Numerical optimisation was conducted using a D-optimal design to determine the optimal conditions for the esterification of SFOUFA with TMP. The parameters involved in this study were varied within a predefined range to achieve the highest possible response, which in this case is the percentage yield of SFOUFATMPE. A higher desirability value indicates a better model fit and a more accurate prediction. The optimum settings for parameters A, B, C and D were set within their respective ranges, while the response, SFOUFATMPE percentage yield, was set to be maximal. Based on the D-optimal design, the predicted optimal conditions were a 4.0 mole ratio of SFOUFA to TMP, a catalyst amount of 1.13 wt. %, a reaction time of 6 hours and a reaction temperature of 154 °C. Under these conditions, the model predicted a maximum yield of 80.02 %. The desirability of this predicted model was calculated to be 1.00, indicating that the model output is ideal and perfectly fits the target criteria.

To verify the reliability of the D-optimal model, esterification reactions were carried out using three randomly selected sets of reaction conditions. The predicted values were then compared to the actual experimental results. Residual standard error (RSE) was calculated for each set, and results were considered valid only if the RSE value was below 5 %. As shown in Table 4, all RSE values were indeed below this threshold, confirming that the model was accurate and dependable. The actual yield obtained under the optimum predicted condition (SFOUFA : TMP mole ratio of 4.0, catalyst amount of 1.13 wt. %, reaction time of 6 hours and reaction temperature of 154 °C) was 79.41 %. The model predicted a yield of 80.02 %, and the calculated RSE for this condition was just 0.76 % (Table 5). This further validates that the D-optimal design provided highly accurate predictions, confirming the robustness and reliability of the optimisation model used in this study.

Table 4. Actual, predicted and RSE value of SFOUFATMPE yield for verification model

Parameter				Yield, %		
A	B, wt. %	C, h	D, °C	actual	predicted	RSE
3.5	1.5	6	159	75.90	77.10	1.56
4.5	3	3	170	74.83	74.20	0.85
3.0	3	7	130	51.16	50.09	2.14

Table 5. Actual, predicted and RSE value of SFOUFATMPE yield for optimal condition

Parameter				Yield, %		
A	B, wt. %	C, h	D, °C	actual	predicted	RSE
4.0	1.13	6	154	79.41	80.02	0.76

3.4 Structural characterisation of biolubricant

The ester composition in the SFOUFATMPE was determined using gas chromatography-flame ionisation detection. The chromatogram in Figure 4 showed triester peaks within the retention time

range of 44 to 47 minutes, which is comparable to the standard ester, with retention peaks in the range of 42 to 48 minutes. This indicates 100 % conversion of the ester. FTIR analysis was used to confirm the structural transformation of SFOUFA (starting material) into SFOUFATMPE after the esterification process, as shown in Figure 5. In the SFOUFA spectrum, the presence of carboxylic acid functional groups was indicated by a broad O–H stretching band between 3000 and 3400 cm^{-1}, a C=O stretching vibration at 1708 cm^{-1} and C–O stretching bands at 1290 and 1248 cm^{-1} [16,17]. The aliphatic C–H stretching of sp^3-hybridised carbons was noticed at 2923 and 2854 cm^{-1}, while the sp^2 C–H stretching appeared at 3008 cm^{-1}. After esterification, the FTIR spectrum of SFOUFATMPE showed the disappearance of the O–H band, confirming the conversion of carboxylic acids to esters. A strong C=O stretching band for esters was shifted to 1740 cm^{-1}, and new C–O stretching bands were noticed at 1238 and 1160 cm^{-1}. The retention of C–H bands at 2923, 2854 and 3008 cm^{-1} indicated that the hydrocarbon chain and unsaturation remained intact [18]. These confirm the successful formation of SFOUFATMPE through the esterification process.

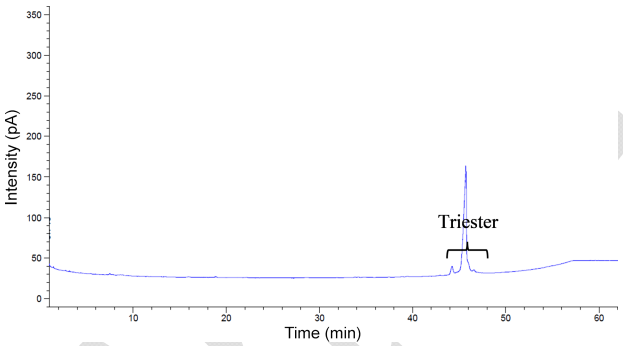

Figure 4. Chromatogram of SFOUFATMPE for triester

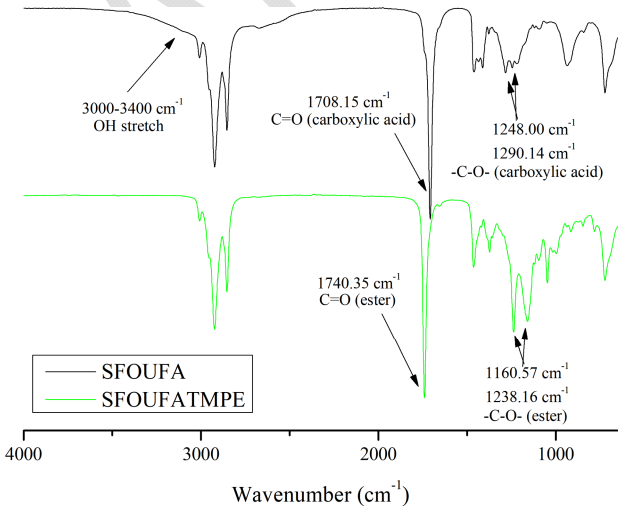

Figure 5. FTIR spectra of SFOUFA and SFOUFATMPE

NMR spectroscopy was used to elucidate the molecular structure of SFOUFATMPE through both proton (^1H) and carbon (^{13}C) spectra. The ^1H NMR spectrum, as presented in Figure 6, reveals several characteristic chemicals and is summarised in Table 6. The peak noticed at 0.86 – 0.90 ppm corresponds to the methyl group (–CH_3), and the peak at 1.23 – 1.36 ppm corresponds to the methylene group (–CH_2–) along the aliphatic chains. Peaks at 1.58 – 1.61 ppm correspond to the methylene groups adjacent to carbonyl groups (–CO–CH_2–CH_2–) and peaks at 1.98 – 2.07 ppm correspond to allylic methylene protons (–CH=CH–CH_2–). The peak at 2.27 – 2.31 ppm corresponds to the methylene protons adjacent to the carbonyl group (–CO–CH_2–), and the peak at 2.75 – 2.78 ppm corresponds to bis-allylic protons (=CH–CH_2–CH=). A peak at 4.12 – 4.14 ppm corresponds to methylene protons bonded to oxygen atoms (–CH_2–O–) within the TMP backbone. The peak at 5.30 – 5.38 ppm corresponds to vinylic protons (–CH=CH–). Additionally, a peak at 7.28 ppm corresponds to the solvent, deuterated chloroform ($CDCl_3$) [16]. The noticed chemical shifts were in agreement with those reported by Pavia et al. [16].

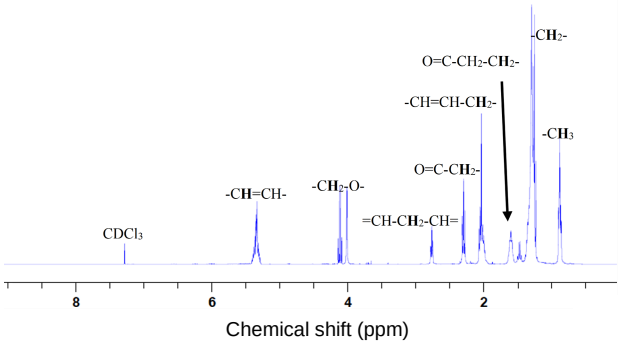

Figure 6. ^1H NMR spectrum of SFOUFATMPE

Table 6. The chemical shift for ^1H NMR spectrum of SFOUFATMPE

Type of proton	Chemical shift, ppm	
	SFOUFATMPE	Pavia et al. [16]
–CH_3	0.86 – 0.90	0.7 – 1.3
–CH_2–	1.23 – 1.36	1.2 – 1.4
O=C–CH_2–CH_2–	1.58 – 1.61	1.5 – 2.0
–CH=CH–CH_2–	1.98 – 2.07	1.6 – 2.6
O=C–CH_2–	2.27 – 2.31	2.1 – 2.5
=CH–CH_2–CH=	2.75 – 2.78	2.5 – 3.0
–CH_2–O– (TMP)	4.12 – 4.14	4.0 – 4.5

The ^{13}C NMR spectrum, shown in Figure 7 and summarised in Table 7, further supports the structural assignment. Peaks at 8.12 ppm and 14.02 – 14.15 ppm correspond to methyl carbons ($-CH_3$), while signals in the range of 20.96 – 31.88 ppm correspond to methylene carbons ($-CH_2-$). The peak noticed at 33.80 – 34.24 ppm corresponds to carbon atoms adjacent to carbonyl groups ($-CO-CH_2-$). A peak at 40.59 ppm is attributed to the quaternary carbon (–C–) of the TMP backbone and a peak at 63.67 ppm confirms the presence of $-CH_2-O-$ groups that come from the TMP structure. The solvent peak for $CDCl_3$ appears at 77.00 ppm. The presence of olefinic carbons (–C=C–) is indicated by a peak at 127.88 – 130.15 ppm, while a strong peak at 173.42 ppm corresponds to the ester carbonyl carbon (–COOR) [16], confirming the successful formation of the ester functional group in SFOUFATMPE.

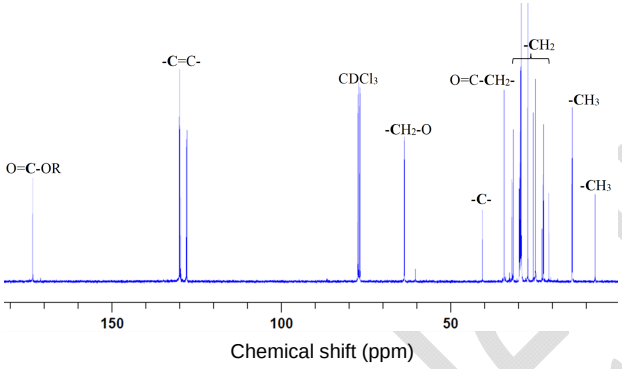

Figure 7. ^{13}C NMR spectrum of SFOUFATMPE

Table 7. The chemical shift for ^{13}C NMR spectrum of SFOUFATMPE

Type of carbon	Chemical shift, ppm	
	SFOUFATMPE	Pavia et al. [16]
$-CH_3$ (TMP)	8.12	8 – 30
$-CH_3$	14.02 – 14.15	8 – 30
$-CH_2-$	20.96 – 31.88	15 – 55
$O=C-CH_2$	33.8 – 34.24	15 – 55
–C– (TMP)	40.59	20 – 60
$-CH_2-O-$ (TMP)	63.67	40 – 80
–C=C–	127.88 – 130.15	100 – 150
O=C–OR (ester)	173.42	155 – 185

3.5 Physicochemical properties of biolubricant

The lubrication properties of SFOUFATMPE were determined using a slightly modified method from Borugadda and Goud [18] and Abd Wafti et al. [19]. The key parameters assessed included flash point, pour point, kinematic viscosity, viscosity index and oxidative stability. The results of these tests are presented in Table 8. The pour point of a lubricant is significantly influenced by the degree of unsaturation in its fatty acid composition. In this study, sunflower oil (SFO), which contains a high proportion of unsaturated fatty acids such as oleic and linoleic acids, exhibited a pour point of −13 °C. Following the chemical modification to produce SFOUFATMPE, the pour point further decreased to −18 °C. This improvement is primarily attributed to the presence of unsaturated fatty acids, whose double bonds introduce kinks in the hydrocarbon chains, disrupting orderly molecular packing and thereby inhibiting crystallisation at low temperatures. Generally, lower pour points are noticed in polyolesters synthesised from shorter-chain saturated fatty acids (C4–C12) or those with a higher content of unsaturated fatty acids, due to similar molecular disordering effects [20]. The high degree of unsaturation in the SFOUFA starting material plays a critical role in enhancing the cold-flow properties of the resulting ester.

Table 8. Physicochemical properties of SFO and SFOUFATMPE

Property	Method	SFO	SFOUFA-TMPE
Pour point, °C	ASTM D97	– 13	– 18
Flash point, °C	ASTM D93	280	290
Viscosity at 40 °C, mm^2/s	ASTM D445	30.54	32.47
Viscosity at 100 °C, mm^2/s	ASTM D445	7.22	7.21
Viscosity Index	ASTM D2270	212	195
Oxidative stability, min	ASTM D2272	22	24

The flash point is a critical indicator of a lubricant's thermal stability and volatility [21], with higher values indicating improved resistance to ignition at elevated temperatures. In this study, SFO had a flash point of 280 °C, while its modified ester, SFOUFATMPE, exhibited a higher flash point of 290 °C. The fatty acid chains in SFOUFATMPE range from C16 to C18 in length, contributing to its high flash point. Longer carbon chains generally increase molecular weight and reduce volatility, thereby requiring more energy for vapourisation and ignition. The flash point of SFOUFATMPE not

only exceeds the ester-based requirement but also aligns with that of petroleum-based lubricants. This highlights the effectiveness of chemical modification in enhancing thermal stability and supports the potential of SFOUFATMPE as a sustainable, high-performance biobased lubricant for use in high-temperature industrial environments.

The kinematic viscosity of SFOUFATMPE was measured as 32.47 mm^2/s at 40 °C and 7.21 mm^2/s at 100 °C, placing it in ISO VG 32 viscosity grade according to ISO 3448. This viscosity range makes it suitable for use in hydraulic systems, compressors and general industrial machinery, where moderate viscosity and stable flow characteristics are essential. Compared with SFO, which exhibited viscosities of 30.44 mm^2/s at 40 °C and 7.22 mm^2/s at 100 °C, the values are similar. This similarity occurs because SFOUFATMPE retains the structural characteristics of the original triacylglycerol, mimicking its molecular backbone through the formation of three ester linkages with TMP. The preserved structural arrangement contributes to comparable viscosity behaviour, while the polyolester structure enhances thermal and oxidative stability, making SFOUFATMPE a more reliable biolubricant for ISO VG 32 applications.

The oxidative stability of a lubricant reflects its resistance to degradation in the presence of oxygen, which is critical for maintaining performance during long-term use, especially at elevated temperatures. In this study, SFO exhibited an oxidative stability of 22 minutes, whereas the modified ester, SFOUFATMPE, showed a slightly improved stability of 24 minutes. This enhancement is attributed to the absence of β-hydrogen atoms in the TMP backbone used in the esterification process. In contrast, the glycerol backbone present in SFO contains β-hydrogen atoms, which are susceptible to oxidative attack, leading to degradation [5]. By replacing glycerol with a more stable TMP structure, the resulting ester exhibits greater oxidative resistance, contributing to improved long-term performance and reliability of the lubricant under oxidative conditions.

3.6 Rheology of biolubricant

The rheological behaviour of SFOUFATMPE was evaluated by plotting shear stress and viscosity versus shear rate, as shown in Figure 8. The shear stress-shear rate curve (Fig. 8a) displays a linear trend indicating a direct proportionality between shear stress and shear rate. This linearity demonstrates that SFOUFATMPE behaves as a Newtonian fluid, with viscosity independent of the applied shear rate. Correspondingly, the viscosity-shear rate curve (Fig. 8b) shows an initially unstable region at low shear rates due to structural adjustment of the fluid, followed by a constant viscosity over the shear rate range (40 – 100 s^{-1}), indicating uniform molecular interactions and the absence of shear-thinning or shear-thickening effects. This rheological behaviour is advantageous for lubricants as it ensures stable flow and predictable film formation under varying shear conditions [9].

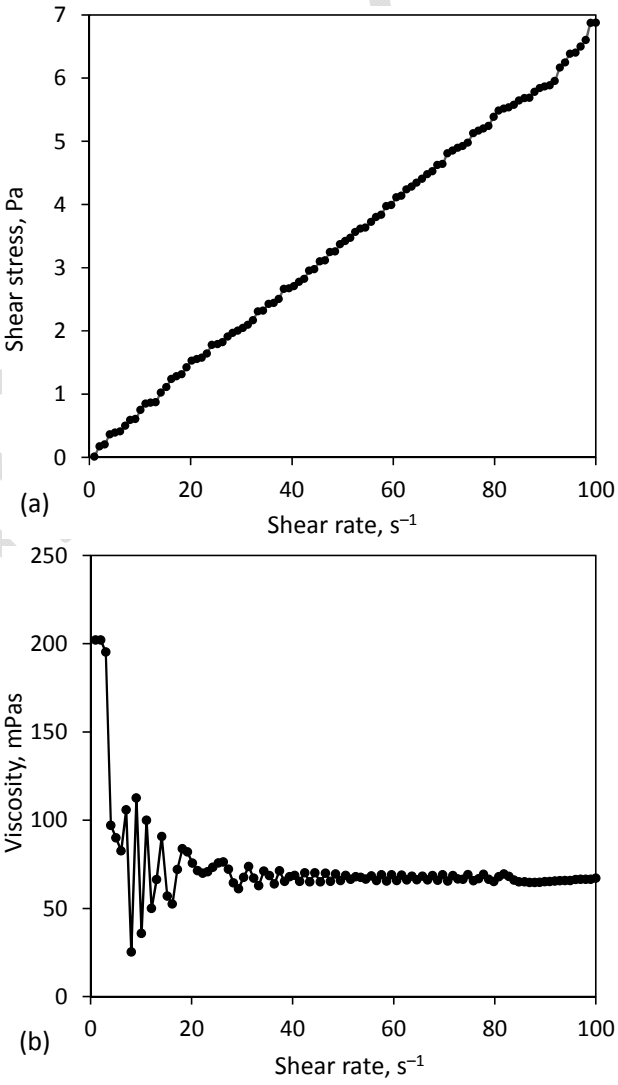

Figure 8. Rheology of SFOUFATMPE: (a) shear stress vs shear rate and (b) viscosity vs shear rate

4. Conclusion

The study demonstrates the successful production of a biolubricant base from renewable SFOUFA through esterification with TMP. The process was optimised using RSM with a D-optimal design, evaluating the effects of mole ratio, catalyst amount, reaction time and reaction temperature.

The best conditions were 4.0 SFOUFA : TMP mole ratio, 1.13 wt. % sulfuric acid catalyst amount, 6 hours reaction time and 154 °C reaction temperature, giving a 79.41 % yield of SFOUFATMPE.

The synthesised biolubricant showed good performance. It had a flash point of 290 °C, indicating strong thermal stability and a pour point of –18 °C, showing excellent low-temperature flow behaviour. However, the oxidative stability of 24 minutes indicates that the product still has limited resistance to oxidation, and further chemical modification is required to improve its performance for commercial applications.

Overall, this work shows that sunflower oil-based fatty acids can be converted into a biolubricant through an efficient and optimised process. Using plant-based, biodegradable and renewable feedstock supports the development of greener, more sustainable lubricant alternatives to petroleum-based products.

Acknowledgement

Special appreciations are extended to the Ministry of Higher Education for the financial support received through the research grant Fundamental Research Grant Scheme – Early Career Researcher (FRGS-EC) (Grant no. FRGS-EC/1/2024/STG04/UITM/02/20) and for the MyBrainSc scholarship. The authors express their gratitude for the invaluable research facilities generously provided by Universiti Teknologi MARA (UiTM) Kampus Kuala Pilah.

References

[1] H. Guo, A.R. Adukure, P. Iglesias, Effect of ionicity of three protic ionic liquids as neat lubricants and lubricant additives to a biolubricant, Coatings, Vol. 9, No. 11, 2019, Paper 713, DOI: 10.3390/coatings9110713

[2] J.L. Teh, R. Walvekar, K.C. Ho, M. Khalid, Biolubricants from waste cooking oil: A review of extraction technologies, conversion techniques, and performance enhancement using natural antioxidants, Journal of Environmental Management, Vol. 375, 2025, Paper 124267, DOI: 10.1016/j.jenvman.2025.124267

[3] M.A.I. Malik, M.A. Kalam, M.A. Mujtaba, F. Almomani, A review of recent advances in the synthesis of environmentally friendly, sustainable, and nontoxic bio-lubricants: Recommendations for the future implementations, Environmental Technology & Innovation, Vol. 32, 2023, Paper 103366, DOI: 10.1016/j.eti.2023.103366

[4] R.S. Situmorang, A.A.C. Saragih, C.P.A. Hutauruk, J. Haryanto, W. Simanullang, A. Irwan, H.V. Sihombing, W.F. Simanullang, Y. Oishi, Synthesis and characterisation of palm oil-based biolubricant for application as cutting fluid, Tribology and Materials, Vol. 4, No. 4, 2025, pp. 192-200, DOI: 10.46793/tribomat.2025.018

[5] M.M. Khairuddin, A. Abdullah, N.M. Nor, Synthesis and characterization of sunflower oil unsaturated fatty acid pentaerythritol ester as green biolubricant base stock, Malaysian Journal of Chemistry, Vol. 26, No. 3, 2024, pp. 373-382.

[6] Y.-N. Lye, N. Salih, J. Salimon, Optimization of partial epoxidation on *Jatropha curcas* oil based methyl linoleate using urea-hydrogen peroxide and methyltrioxorhenium catalyst, Applied Science and Engineering Progress, Vol. 14, No. 1, 2021, 89-99, DOI: 10.14416/j.asep.2020.12.006

[7] S. Wu, T. Sun, Z. Cai, J. Shen, W. Yang, Z. Zhao, D. Yang, Biolubricant base stock with improved low temperature performance: Ester complex production using housefly (*Musca domestica* L.) larval lipid, Renewable Energy, Vol. 162, 2020, pp. 1940-1951, DOI: 10.1016/j.renene.2020.10.001

[8] N.M. Nor, D. Derawi, J. Salimon, Esterification and evaluation of palm oil as biolubricant base stock, Malaysian Journal of Chemistry, Vol. 21, No. 2, 2019, pp. 28-35.

[9] N.M. Nor, N. Salih, J. Salimon, Optimization and lubrication properties of Malaysian crude palm oil fatty acids based neopentyl glycol diester green biolubricant, Renewable Energy, Vol. 200, 2022, pp. 942-956, DOI: 10.1016/j.renene.2022.09.112

[10] F.I. Jamaluddin, M.M. Khairuddin, A. Abdullah, N.M. Nor, Synthesis of TMP ester via esterification of corn oil fatty acids and trimethylolpropane as a potential biolubricant base stock, Malaysian Journal of Chemistry, Vol. 26, No. 3, 2024, pp. 312-319.

[11] F.J. Ramos, J.C. de Haro, J.F. Rodríguez, Á. Pérez, M. Carmona, Predicting the viscosity of ester biolubricants by the functional groups of their compounds using a sensitivity parameter model, Lubricants, Vol. 13, No. 4, 2025, Paper 179, DOI: 10.3390/lubricants13040179s

[12] S.M.A. Rahman, P. Sharma, Z. Said, Application of response surface methodology based D-optimal design for modeling and optimisation of osmotic dehydration of Zucchini, Digital Chemical Engineering, Vol. 4, 2022, Paper 100039, DOI: 10.1016/j.dche.2022.100039

[13] A. Pattanaik, V. Rayasam, Analysis of reverse cationic iron ore fines flotation using RSM-D-optimal design – An approach towards

sustainability, Advanced Powder Technology, Vol. 29, No. 12, 2018, pp. 3404-3414, DOI: 10.1016/j.apt.2018.09.021
[14] M.M. Khairuddin, A. Abdullah, N.N. Dzulkifli, N.M. Nor, Optimization of sunflower oil hydrolysis using the D-optimal design, Malaysian Journal of Analytical Sciences, Vol. 27, No. 5, 2023, pp. 1062-1078.
[15] M.M. Khairuddin, A. Abdullah, N.F. Norshahimy, M.A.M. Sa'ad, N.M. Nor, Separation of unsaturated and saturated fatty acids from sunflower oil via low-temperature methanol crystallization method, Malaysian Journal of Chemistry, Vol. 27, No. 3, 2025, pp. 224-236.
[16] D.L. Pavia, G.M. Lampman, G.S. Kriz, J.R. Vyvyan, Introduction to Spectroscopy, Cengage Learning, Stamford, 2015.
[17] D. Derawi, J. Salimon, Palm olein based biolubricant basestocks: Synthesis, characterisation, tribological and rheological analysis, Malaysian Journal of Analytical Sciences, Vol. 17, No. 1, 2013, pp. 153-163.
[18] V.B. Borugadda, V.V. Goud, Response surface methodology for optimization of bio-lubricant basestock synthesis from high free fatty acids castor oil, Energy Science & Engineering, Vol. 3, No. 4, 2015, pp. 371-383, DOI: 10.1002/ese3.77
[19] N.S. Abd Wafti, R. Yunus, H.L.N. Lau, T.S.Y. Choong, S. Abd-Aziz, Enzymatic synthesis of palm oil-based trimethylolpropane ester as biolubricant base stock catalyzed by Lipozyme 435, Energy, Vol. 260, 2022, Paper 125061, DOI: 10.1016/j.energy.2022.125061
[20] S.K. Tulashie, F. Kotoka, The potential of castor, palm kernel, and coconut oils as biolubricant base oil via chemical modification and formulation, Thermal Science and Engineering Progress, Vol. 16, 2020, Paper 100480, DOI: 10.1016/j.tsep.2020.100480
[21] F.J. Owuna, Stability of vegetable based oils used in the formulation of ecofriendly lubricants – A review, Egyptian Journal of Petroleum, Vol. 29, No. 3, 2020, pp. 251-256, DOI: 10.1016/j.ejpe.2020.09.003